EFFECTS OF THERMAL GRADIENTS ON DEFECT FORMATION DURING THE CONSOLIDATION OF PARTIALLY-IMPREGNATED PREPREGS

Timotei Centea[1], Garrett Peters[2], Karissa Hendrie[1], and Steven R. Nutt[2]

[1] Department of Aerospace and Mechanical Engineering, University of Southern California, 3651 Watt Way, VHE-416, Los Angeles, CA 90089-0241, USA, centea@usc.edu

[2] Department of Chemical Engineering and Materials Science, University of Southern California, 3651 Watt Way VHE-602, Los Angeles, CA 90089-0241, nutt@usc.edu

Abstract: We describe the effects of thermal gradients on the consolidation of partially-impregnated prepregs. Laminates were cured on a heated tool in isothermal and non-isothermal conditions. Key process parameters were varied, including thermal gradient magnitude, air evacuation direction, and vacuum quality. Laminate quality was assessed using microscopy of polished cross-sections and x-ray computed tomography, and interpreted relative to the evolution of resin and prepreg properties during cure. The results show that thermal gradients influenced the rate of impregnation of the prepreg and the rate of gas transport, and affected the amount and distribution of porosity when air was not fully evacuated. Temperature distributions that led to cold regions at the ply boundaries were advantageous, typically exhibiting lower porosity than isothermal baselines. Conversely, gradients resulting in hotter-than-average part perimeters effectively sealed air within the laminate, degrading quality. The results clarify fundamental defect formation mechanisms for partially-impregnated prepregs and other processes reliant on air evacuation through an unsaturated preform, and provide guidelines for part, tool, and process design.

Please cite the article as: T. Centea, G. Peters, K. Hendrie and S.R. Nutt, **"Effects of Thermal Gradients on Defect Formation During Consolidation of Partially-Impregnated Prepregs"** J. Compos Mat 51 [28] (2017) 3987-4003 DOI: **10.1177/0021998317733317**

INTRODUCTION

The traditional manufacturing route for structural composites is autoclave processing of prepregs [1]. Prepreg plies, or layers of fiber reinforcement pre-impregnated with a catalyzed but uncured thermoset resin, are first stacked on a tool to build up a laminate. Then, they are enclosed within a consumable assembly that forms a vacuum bag, and cured within a pressurized, heated autoclave vessel. The pressure difference across the vacuum bag provides the driving force for consolidation of the laminate, compacting the fiber bed, driving resin into unsaturated regions, and suppressing the evolution of volatiles and formation of porosity and other defects. Concurrently, the imposed thermal cycle promotes resin polymerization/cross-linking (cure), converting the matrix from a viscous fluid into a stiff, glassy solid.

Autoclave processing enables fabrication of consistent, high-value aerospace parts, and the capacity to ensure low defect levels has long justified several disadvantages, including high capital and operating costs (particularly for large pressure vessels) and limits on production throughput, part size, and subcontractor choices [2]. However, the growing and diversifying use of composites has also motivated development of a broad range of out-of-autoclave (OoA) processes that can accommodate a wider range of part characteristics, cost requirements, production rates, and life cycle environmental impact targets.

Manufacture of high-performance composites without an autoclave can be carried out using different approaches, including vacuum bag-only (VBO) consolidation and higher-pressure methods such as resin transfer molding (RTM) and press molding. The product forms of the fiber and resin materials, physical phenomena that govern processing and defect formation, and suitable applications (based on technical and economic criteria) can vary between these approaches.

Please cite the article as: T. Centea, G. Peters, K. Hendrie and S.R. Nutt, **“Effects of Thermal Gradients on Defect Formation During Consolidation of Partially-Impregnated Prepregs”** J. Compos Mat 51 [28] (2017) 3987-4003 DOI: **10.1177/0021998317733317**

However, broadly, VBO consolidation enables the cost-effective production of larger parts while being susceptible to defect formation due to a pressure limit of approx. 0.1 MPa. Several VBO approaches have been developed, including VBO prepregs, resin film infusion, and vacuum-assisted resin infusion/resin transfer molding (VARI or VARTM). These methods utilize different product forms for the initial constituents, and rely on flow over varying lengths. However, in all cases, defect control requires the evacuation of entrapped air through permeable, dry regions of the fiber bed, and the subsequent saturation of the reinforcement by resin [3]. Conversely, higher-pressure methods such as RTM and press molding rely on high consolidation pressures (>0.1 MPa) to achieve consistently high part quality, but require expensive infrastructure and tooling investments that impose economic limits on part size.

Vacuum bag-only (VBO) prepregs allow the OoA production of structural composites using protocols similar to autoclave cure. The material properties, process phenomena, and manufacturing considerations associated with such materials have been reviewed [4]. VBO prepregs feature a partially-impregnated initial microstructure containing both dry and resin-rich regions. The dry regions consist of fiber tow cores, and allow in-plane air removal during a room-temperature vacuum hold prior to the onset of cure. Then, at elevated temperature (oven, heated blanket, or heated tool) and under vacuum compaction, the dry regions are infiltrated by surrounding resin. This consolidation process is effective in many cases, as described in a recent review article [4]. However, in the absence of a high pressure safeguard, key phenomena can be affected by material and process factors, including temperature cure cycle, vacuum quality and location (particularly within large bags), prepreg state (out-time and moisture content), and part characteristics such as geometry, size and layup [4]. Consequently, the successful, efficient, and consistent production of large composite structures using VBO methods requires science-based defect mitigation strategies that address manufacturing challenges and improve process control.

Thermal Gradients

Thermal gradients can occur during composite fabrication due to non-uniform part and tool geometries, spatial variations in heat transfer, or a localized resin exotherm. Gradients frequently form during heat-up, and contribute to maximum acceptable heat-up rates of about 3 – 5°C/min in convective environments. However, they can also occur at steady-state. In-plane gradients can arise due to large-scale differences in convective heat transfer within an autoclave or oven, while through-thickness non-uniformities can occur due to a significant offset between tool and external temperatures. Uneven heating is usually considered undesirable because temperature influences resin behavior and defect levels. Colder part regions experience slower cure and can increase the minimum required cycle time. Conversely, hotter areas are vulnerable to runaway exotherms, excessive resin flow, and matrix degradation. Generally, gradients can lead to non-uniformities in flow, compaction, defect levels, mechanical properties, and part dimensions.

In recent decades, non-isothermal cure has largely been discussed within the context of process simulations for autoclave cure (e.g., [5–7]) and resin transfer molding (e.g., [8–17]). These studies have focused primarily on developing models that capture the effects of local temperature on resin thermochemical and thermomechanical properties, and that predict the impact of spatial variations on large-scale fluid migration within preforms, and the formation of residual stresses. However, few studies have assessed the effects of thermal gradients on the formation of microstructural defects during low-pressure, vacuum-driven processing.

Please cite the article as: T. Centea, G. Peters, K. Hendrie and S.R. Nutt, **"Effects of Thermal Gradients on Defect Formation During Consolidation of Partially-Impregnated Prepregs"** J. Compos Mat 51 [28] (2017) 3987-4003 DOI: **10.1177/0021998317733317**

In principle, VBO prepreg processing and other manufacturing methods that rely solely on vacuum-assisted consolidation are particularly vulnerable to thermal gradients because the defect suppression mechanisms are strongly temperature-dependent. Resin flow into dry fiber regions governs the progressive decrease of the laminate in-plane permeability [18]. Hence, in addition to traditional thermally-induced defects (e.g., residual stresses, resin degradation), thermal gradients can potentially affect the capacity and direction of in-plane gas transport and impact the amount and spatial distribution of porosity.

Thermal gradient issues can be investigated – and potentially addressed in practice – by leveraging the ability to manufacture outside of the autoclave. VBO prepregs are most often cured within convection ovens. However, heat can also be imparted conductively using integrally heated tools and heating blankets (as summarized by Black [19]) or through a higher-density heat transfer fluid (e.g., QuickStep). Such infrastructure can improve thermal efficiency and heat-up/cool-down rates, potentially leading to lower energy costs [20]. More importantly, direct heating through tooling can sometimes enable local control over heat transfer, allowing the mitigation (or strategic use) of thermal gradients. The design and viability of heated tool cure has been discussed by Grove and colleagues [21–23], O'Bradaigh et al. [24], Smith et al. [25] and Payette et al. [26]. However, so far, studies have not directly assessed the effects of spatially non-uniform temperature fields on processing phenomena and final part quality.

OBJECTIVES AND APPROACH

We studied the influence of thermal gradients on the processing of partially-impregnated prepregs cured using VBO methods. Our objectives were: (1) to determine the effects of in-plane thermal non-uniformity on the consolidation of a partially-impregnated prepreg and on the cured part

Please cite the article as: T. Centea, G. Peters, K. Hendrie and S.R. Nutt, **"Effects of Thermal Gradients on Defect Formation During Consolidation of Partially-Impregnated Prepregs"** J. Compos Mat 51 [28] (2017) 3987-4003 DOI: **10.1177/0021998317733317**

microstructure, and (2) to assess whether heated tooling (and/or other advanced curing environments allowing localized heat transfer) offer opportunities for exploiting non-uniform temperature distributions.

A lab-scale, multi-zone heated tool was used to manufacture laminates from partially-impregnated VBO prepregs. A variety of thermal configurations were studied, and pressure was varied by modifying the vacuum level and by allowing or restricting air evacuation at laminate boundaries. The microstructural quality of the laminates was evaluated by assessing the amount and distribution of porosity, and correlated to resin and prepreg behavior. The resulting dataset captured the influence of thermal gradients on air removal, resin flow, and porosity formation. Moreover, the data also clarified the sensitivity of VBO cure to spatial variations in temperature, and highlighted the potential use of thermal gradients to control defects. Overall, the study contributes to the growing body of knowledge on OoA manufacturing methods capable of yielding high quality composites, including VBO prepregs, RFI, and VARTM/VARI.

METHODS

Heated Tool

The heated tool used within this study was designed and fabricated in-house as a research test bed [27], and is shown in Figure 1. The tool consists of six independent cells (100 mm × 100 mm) arranged in a linear pattern and overlaid by a uniform flat aluminum tool plate. Each cell is composed of an aluminum heat sink, four embedded resistive cartridge heaters, a cooling fan and two thermocouples. The resistive cartridges (McMaster-Carr, 300W, 240V) enable rapid heating of the tool surface, while the cooling fans (McMaster-Carr, 160 CFM, 12 V DC) and the heat sinks allow rapid convective cooling. The thermocouples are located near the tool surface and are used

Please cite the article as: T. Centea, G. Peters, K. Hendrie and S.R. Nutt, **“Effects of Thermal Gradients on Defect Formation During Consolidation of Partially-Impregnated Prepregs”** J. Compos Mat 51 [28] (2017) 3987-4003 DOI: **10.1177/0021998317733317**

for measurement and control. The heating and cooling systems within each cell are independently controlled through solid state relays (DigiKey DRA1-MCX240D5) by a digital acquisition and control system (National Instruments cRIO) and a virtual instrument (National Instruments LabView). A PC interface allows cure cycles to be defined in terms of ramps and dwells, and records measured data.

The performance of the heated tool was evaluated [27]. The system is capable of rapid heating (up to 30°C/min) and accurate (± 1.5°C) temperature control between 30°C and 200°C. The system is also capable of maintaining steady-state thermal gradients (using concurrent heating and cooling) of up to 30°C between adjacent cells. As a result, VBO cure is viable in both isothermal and non-isothermal conditions.

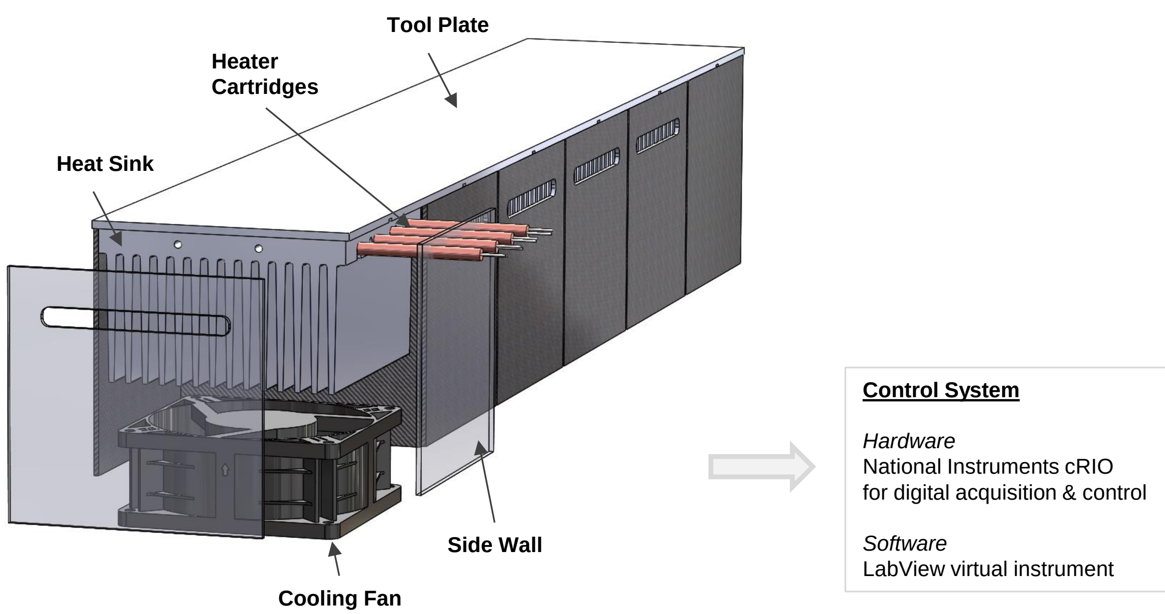

Figure 1: Schematic illustration of the multi-zone heated tool.

Materials

Laminates were manufactured using a commercially-available VBO prepreg made up of thermoset resin and unidirectional carbon fiber tape (Cycom 5320-1/IM7, Cytec Industries). The 5320-1 system is a toughened epoxy designed for vacuum bag-only cure between 93°C and 121°C (with 0.56-2.77°C/min ramps) followed by post-cure at 177°C. The unidirectional fiber bed has an areal weight of 145 g/m^2. The prepreg has a resin content of 33% by weight, and a manufacturer-specified out-life of 30 days. The material used in this study was extracted from a single roll/batch for which the properties and uniformity were confirmed by a manufacturer-supplied certification sheet, minimizing the likelihood of variability in resin degree of cure or fiber bed saturation. The prepreg roll was stored in a freezer (-10°C), and had an estimated accrued out-time of 4 days.

The 5320-1 system has served as a test case for numerous studies on VBO prepreg processing. Predictive models are available for the cure kinetics and viscosity of 5320-1 as a function of time, temperature, and out-time [28]. Moreover, thermogravimetric analysis has shown that 5320-1 exhibits less than 0.5% mass loss up to 280°C [28], indicating that the resin does not release significant amounts of volatile organic compounds (VOCs) or vaporized moisture. The mechanisms of process-induced void formation during cure with spatially-uniform temperature have also been evaluated [4], providing useful baselines for the current study. The 5320-1/UD prepreg is partially impregnated [29], with the dry fiber tow cores used for air evacuation and porosity control prior to impregnation at elevated temperature. The through-thickness permeability of VBO prepregs of the same type is negligible (or non-existent) [30], indicating that air evacuation occurs primarily in-plane. Restricted air evacuation, sub-optimal pressure conditions, or out-time can lead to porosity, which is located predominantly within fiber tows for this fiber bed

Please cite the article as: T. Centea, G. Peters, K. Hendrie and S.R. Nutt, **"Effects of Thermal Gradients on Defect Formation During Consolidation of Partially-Impregnated Prepregs"** J. Compos Mat 51 [28] (2017) 3987-4003 DOI: **10.1177/0021998317733317**

architecture [29,31]. Without process deviations, 5320-1/UD laminates have been shown to exhibit low microstructural defect levels (< 0.5% porosity) across a wide range of cure temperatures [32], providing a useful reference and lower bound for porosity observed in this study.

Laminate Manufacture

Laminates measuring 75 mm × 300 mm (± 5 mm) and composed of twelve plies were fabricated to investigate the influence of three potentially interacting parameters: thermal gradient magnitude, in-plane air removal direction, and vacuum quality (Table 1). Figure 2 shows schematics of the thermal and air evacuation conditions. Two baseline, manufacturer-recommended cure dwells were assessed: 93°C for 12 h, and 121°C for 3 h (Figure 2A). Heat-up rates consisted of 1.5°C/min for the 121°C regions, and 1.1°C/min for the 93°C regions (to reach the dwell in the same amount of time).

Table 1:Summary of test laminates, their processing conditions, and their function.

#	Thermal Condition	Temperature	Gradient Magnitude	Air Evacuation Direction	Vacuum Level	Purpose
1	Isothermal	93°C	N/A	N/A	100%	Baseline for 1D air evacuation
2	Isothermal	121°C	N/A	N/A	100%	
3	Isothermal	93°C	N/A	N/A	75%	
4	Isothermal	121°C	N/A	N/A	75%	
5	Isothermal	93°C	N/A	N/A	25%	
6	Isothermal	121°C	N/A	N/A	25%	
7	Gradient	93°C - 121°C	0.09°C/mm	Cold-Side	100%	Effects of thermal gradients with 1D air evacuation
8	Gradient	93°C - 121°C	0.09°C/mm	Cold-Side	75%	
9	Gradient	93°C - 121°C	0.09°C/mm	Cold-Side	25%	
10	Gradient	93°C - 121°C	0.09°C/mm	Hot-Side	100%	
11	Gradient	93°C - 121°C	0.09°C/mm	Hot-Side	75%	
12	Gradient	93°C - 121°C	0.09°C/mm	Hot-Side	25%	
13	Gradient	93°C - 121°C	0.28°C/mm	Cold-Side	100%	
14	Gradient	93°C - 121°C	0.28°C/mm	Cold-Side	75%	
15	Gradient	93°C - 121°C	0.28°C/mm	Cold-Side	25%	
16	Gradient	93°C - 121°C	0.28°C/mm	Hot-Side	100%	
17	Gradient	93°C - 121°C	0.28°C/mm	Hot-Side	75%	
18	Gradient	93°C - 121°C	0.28°C/mm	Hot-Side	25%	

Please cite the article as: T. Centea, G. Peters, K. Hendrie and S.R. Nutt, **"Effects of Thermal Gradients on Defect Formation During Consolidation of Partially-Impregnated Prepregs"** J. Compos Mat 51 [28] (2017) 3987-4003 DOI: **10.1177/0021998317733317**

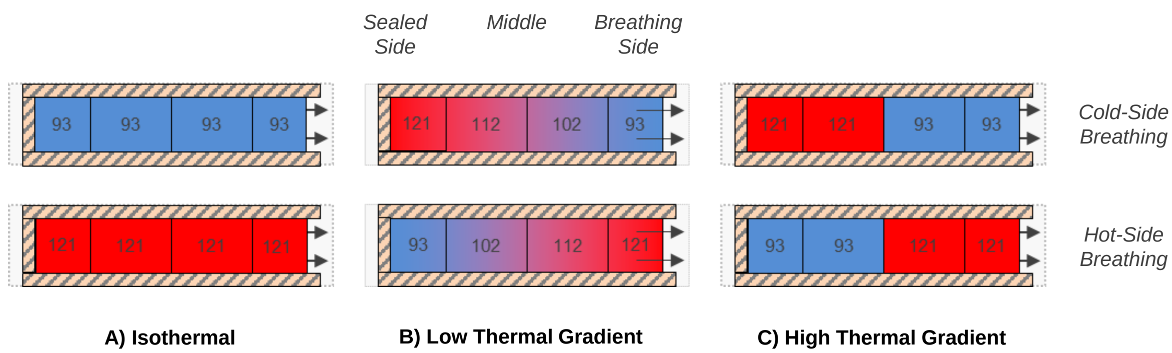

Figure 2: Thermal and edge breathing configurations used for laminate manufacture: including (A) isothermal and non-isothermal conditions with (B) low and (C) high thermal gradients. The vacuum bag sealant tape and consumables are omitted for clarity.

Two non-isothermal cases bounded by these baselines were studied: a low thermal gradient between 93°C and 121°C over four cells, or approx. 0.09°C/mm (measured center-to-center over four cells) (Figure 2B), and a steeper gradient between the same temperatures over one cell, or 0.28°C/mm (Figure 2C). For laminates cured non-isothermally, a 12 h dwell was used to ensure gelation throughout the part. The thermal gradient direction was varied to study coupling with air evacuation by imposing either cold-side breathing or hot-side breathing (Figure 2B and 2C, top and bottom). For cold-side breathing, breathing dams were positioned adjacent to the coldest edge of the laminate, while sealing dams were used on the remaining three sides to restrict air evacuation. Conversely, for hot-side breathing, edge breathing was only applied to the hottest laminate edge. In both cases, because the through-thickness permeability of 5320-based UD prepregs is negligibly low [30] (and given the consumable arrangement described below), the one-dimensional pressure gradient imposed by using only one breathing edge was the sole driving force for air flow. Finally, vacuum quality was varied between to 100% (0 kPa bag pressure), 75%

Please cite the article as: T. Centea, G. Peters, K. Hendrie and S.R. Nutt, **"Effects of Thermal Gradients on Defect Formation During Consolidation of Partially-Impregnated Prepregs"** J. Compos Mat 51 [28] (2017) 3987-4003 DOI: **10.1177/0021998317733317**

(25 kPa) and 25% (75 kPa) to study processing in cases where air remains within the laminate during heated cure. The first two levels span a range that can realistically be encountered in industrial settings, while the latter represents an extreme example intended to accentuate porosity. No room-temperature vacuum hold was imposed prior to cure to capture the effect of resin flow on gas transport. Overall, the test matrix developed for this study allows the effects of non-uniform temperature and pressure conditions to be assessed both in isolation and relative to each other.

Laminates were cured on the heated tool using conventional VBO protocols. The tool surface was covered with a single-use non-perforated fluorinated ethylene propylene (FEP) release film, ensuring that the surface did not change between tests. The prepreg plies were laid up on the first four cells of the heated tool in a $[0°]_{6s}$ stacking sequence, where 0° denotes the fiber direction. Next, edge dams were applied, the laminate was covered with layers of non-perforated FEP film and nylon breather, and the vacuum bag was formed using bagging film and sealant tape. Vacuum was drawn through a port located on the last two cells of the heated tool using a stand-alone pump, and bag pressure was reduced, if needed, using a vacuum regulator and gauge. Heat loss through the top surface (and the formation of through-thickness gradients) was mitigated by using several layers of breather as insulation outside the bag. Prior to this study, thermocouples were placed on the bag-side and tool-side surfaces of a separate laminate to ensure that laminate temperatures corresponded to those imposed by the tool. Layup and bagging were performed by a single person to maximize consistency. The layup conditions were controlled to the extent possible throughout the study, with room temperatures of 22°C ± 2°C and relative humidity levels of 50% ± 10% RH. No major differences in prepreg tack were observed between samples, indicating that ambient conditions did not substantially affect the prepreg material.

The microstructural characteristics of cured laminates were assessed by visual inspection and light microscopy of polished cross-sections (oriented normal to the fiber direction). Laminate thicknesses were measured using a digital micrometer. Then, 50 mm wide samples were extracted from the sealed, middle and breathing regions (Figure 2), and polished on a metallographic grinder/polisher (Buehler MetaServ). The samples were cut from the center of each laminate region, and hence did not include the perimeter (edge). Cross-sectional images were acquired using a video microscope (Keyence VHX-600), and areal void contents were measured through a combination of automatic selection, manual selection and binary thresholding within a scientific image analysis tool (ImageJ).

Finally, the validity of calculating porosity using polished cross-sections was confirmed using X-ray micro-tomography (micro-CT) scans of reference samples with high and low defect levels. Two laminates (5320-1/UD, $[0°]_{6s}$, 127 × 127 mm) were laid up and oven-cured using the higher-temperature (121°C, 3 h) cure cycle. The first part (denoted "breathing") was cured with four breathing edges to minimize defect formation, while the entire perimeter of the second laminate (denoted "sealed") was closed off using sealant tape to restrict air evacuation and maximize defect levels. After cure, a sample from each laminate (25.4 mm × 50.8 mm) was scanned using micro-CT (Nikon Metrology XT S 225 ST, 40 kV, 120 mA, 11.5 μm/pixel). The tomographic data was analyzed by converting reconstructed grayscale images (8 bit) to binary images using a consistent threshold, and determining porosity using two protocols: two-dimensional (2D) void content calculations within 2500 individual planar cross-sections oriented normal to the fiber direction, and three-dimensional (3D) porosity measurement based on pore and solid volumes.

RESULTS

Manufacturing

Thermal History. Thermocouple data recorded during initial testing confirmed that laminate temperatures followed imposed cure cycles, with less than 2°C difference between target and measured temperatures. For all cases, the through-thickness thermal gradient was less than 3°C (and usually smaller), confirming that breather layers placed on top of the bag effectively reduced surface heat loss. This temperature difference is well within the tolerances provided by the prepreg manufacturer, which specifies that the 5320-1 resin can be cured at 121°C ± 5°C. During non-isothermal cure, temperature variations on the surface of each cell were typically less than 3°C, and hence significantly less than those imposed between cells.

Resin and Prepreg Properties. Cure kinetics and viscosity profiles corresponding to 93°C and 121°C cure cycles (the highest and lowest temperatures analyzed in this study) were calculated using published models for the 5320-1 resin [28] (assuming an out-time of four days), and are shown in Figure 3A. The degree of cure (α) began to increase once the temperature reached the isothermal hold. As expected, the resin cured faster at 121°C than at 93°C, and achieved more cure at the end of the cycle (0.70 versus 0.54). The cure rate mismatch substantially affected resin rheology. The minimum viscosity (μ), reached at the end of the heat-up ramp, was significantly less at 121°C than at 93°C (13 Pa·s versus 33 Pa·s). Moreover, gelation occurred 4.5 h earlier, implying that colder laminate regions experienced longer periods of resin and bubble movement.

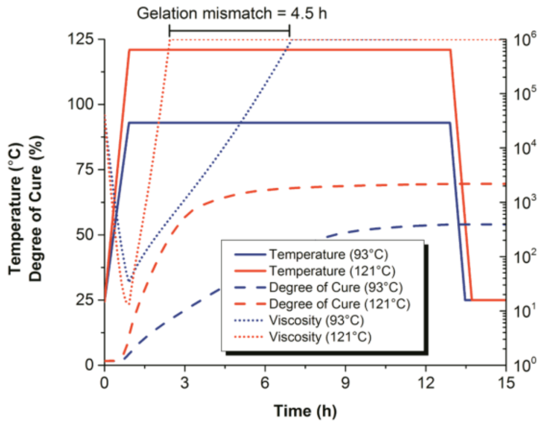

A) Temperature, Degree of Cure and Viscosity

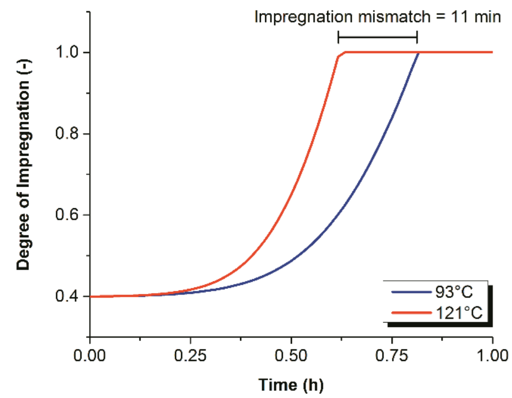

B) Degree of Tow Impregnation

Figure 3: (A) Measured temperature and predicted degree of cure and viscosity data for the 5320-1 resin and cure dwells of 93°C and 121°C. (B) Degree of impregnation of the 5320-1/UD prepreg for 93°C and 121°C cure cycles.

The viscosity mismatch between 93°C and 121°C cycles led to a significant delay in the rate of prepreg impregnation. Flow of a viscous fluid through a porous medium can be modeled using Darcy's Law:

$$\bar{v}_r = -\frac{\bar{\bar{K}}}{\mu(1-V_f)}\nabla P \qquad \text{Eq. (1)}$$

where $\bar{v}_r$ is the average local velocity of the resin within the pore volume, $\bar{\bar{K}}$ is the permeability tensor of the tow, μ is the resin viscosity, V_f is the tow fiber volume fraction, and P is the resin pressure. During VBO prepreg consolidation, the fiber volume fraction, permeability, and resin pressure can evolve due to compaction or relaxation. However, since the process pressure is limited to 0.1 MPa, these changes are likely to have a smaller effect than variations in resin viscosity, which can span several orders of magnitude during cure, and have been shown to correlate strongly with impregnation rates [33]. Within Darcy's Law, the fluid velocity is proportional to the inverse viscosity ($1/\mu$). Hence, the flow number, or the integral sum of the inverse viscosity curve prior to gelation ($t = t_{gel}$) provides a simple, convenient means of comparing resin fluidity between different cure cycles:

$$F_N = \int_{t=0}^{t=t_{gel}} 1/\mu(t)\, dt \qquad \text{Eq. (2)}$$

The 93°C and 121°C cure cycles are associated with flow numbers of 169.2 Pa^{-1} and 253.7 Pa^{-1}, respectively. The 50% increase in flow number for the 121°C cycle, and the lower minimum viscosity at this temperature, show that higher-temperature cure enables faster, more extensive flow – which can be advantageous if the prepreg has incurred high out-time, but which would reduce the prepreg permeability more rapidly than cure at 93°C.

A simple flow model was developed to estimate, in first approximation, the differences in impregnation time versus cure cycle. The derivation and parameter identification steps followed previously-published methodologies for 5320-1 prepregs [33], and are summarized in the Appendix. This simplified model omits some complex aspects of consolidation (e.g., fiber bed compaction/relaxation, flow anisotropy, and edge effects), but accounts for evolving viscosity – and, hence, for the most influential of the parameters present in Eq. (1). The model estimated that tow impregnation progressed faster at 121°C cure than at 93°C, and that full saturation of dry regions occurred 11 min earlier. Thus, laminates cured under gradients experienced spatially non-uniform impregnation during heating, which invariably influenced resin distribution, fiber bed

Please cite the article as: T. Centea, G. Peters, K. Hendrie and S.R. Nutt, **"Effects of Thermal Gradients on Defect Formation During Consolidation of Partially-Impregnated Prepregs"** J. Compos Mat 51 [28] (2017) 3987-4003 DOI: **10.1177/0021998317733317**

saturation, and the capacity for in-plane air evacuation. The results described below will show that, depending on their direction and magnitude, spatial variations either improved or degraded final part quality.

Laminate Properties

Qualitative Observations. Laminates produced under isothermal conditions generally exhibited few surface defects. Hamill et al. [34] studied the mechanisms of surface porosity formation during VBO cure, identifying air entrapment as the major factor and showing that, for a woven fabric prepreg, the amount of surface porosity correlates strongly with vacuum quality. The comparatively limited effect of vacuum quality on surface porosity for the UD prepreg used in this study is attributed to the uniform morphology of the tool-side unidirectional ply and the absence of air entrapment sites (as in Centea and Hubert [29]). Laminates cured non-isothermally exhibited more surface porosity, with hot-side breathing, lower vacuum quality, and higher thermal gradients generally resulting in higher defect levels. These results provided the first indications of how thermal gradients can affect part quality.

The manufactured laminates presented no visible process-induced deformation within the cured state, retaining the flat geometry of the tool. The absence of residual stress effects is attributed to the unidirectional fiber bed architecture and the $[0°]_{6s}$ layup sequence, in which minor errors in the orientation of individual plies are averaged over the relatively large number of total plies ($n = 12$). Note, however, that a detailed study of process-induced deformations (e.g., using a coordinate measuring machine, or CMM) was outside the scope of this study and not performed, and minor geometric deviations may have existed.

Reference Samples. Figure 4 shows X-ray micrographs of the two reference samples (breathing and sealed), along with CT analysis results. The breathing sample exhibited low defect levels. The average porosity (2D), calculated from 2500 cross-sections, was 0.04% (with standard deviation of 0.05%), while the porosity (3D) was determined as 0.02%. Nearly 43% of the planar sections did not exhibit any porosity, and the average characteristic diameter (2D) of detected pores was 14 μm – near the spatial resolution of the CT scan. The sealed sample exhibited extreme porosity, with an average (2D) of 9.26% (with standard deviation of 0.82%) and an actual value (3D) of 9.18%. Every planar cross-section analyzed contained pores, and the average characteristic pore diameter (2D) was 57 μm. Fewer voids were observed in the top (bag-side) and bottom (tool-side) plies of each laminate, which was attributed to favorable air evacuation pathways at the interfaces between the release film, laminate, and metal tool, respectively. Overall, these results indicate that both samples were internally consistent and that the mechanical response of the sealed sample was severely degraded.

The close agreement between 2D (average) and 3D (actual) void contents likely resulted from void morphology. Figure 4B shows that, for this prepreg, fiber bed architecture, and unidirectional stacking sequence, porosity caused by entrapped air manifested as long, needle-like voids oriented along the fiber direction. The ends of each needle-like shape likely consist of regions where loose fiber packing resulted in higher permeability and promoted resin infiltration, sealing off the engineered evacuation pathway of the prepreg. The quasi-cylindrical morphology of the voids decreases the importance of three-dimensional microstructural analysis, enabling void content determination from planar datasets perpendicular to the fiber direction (provided pores are sufficiently smaller than the region of interest).

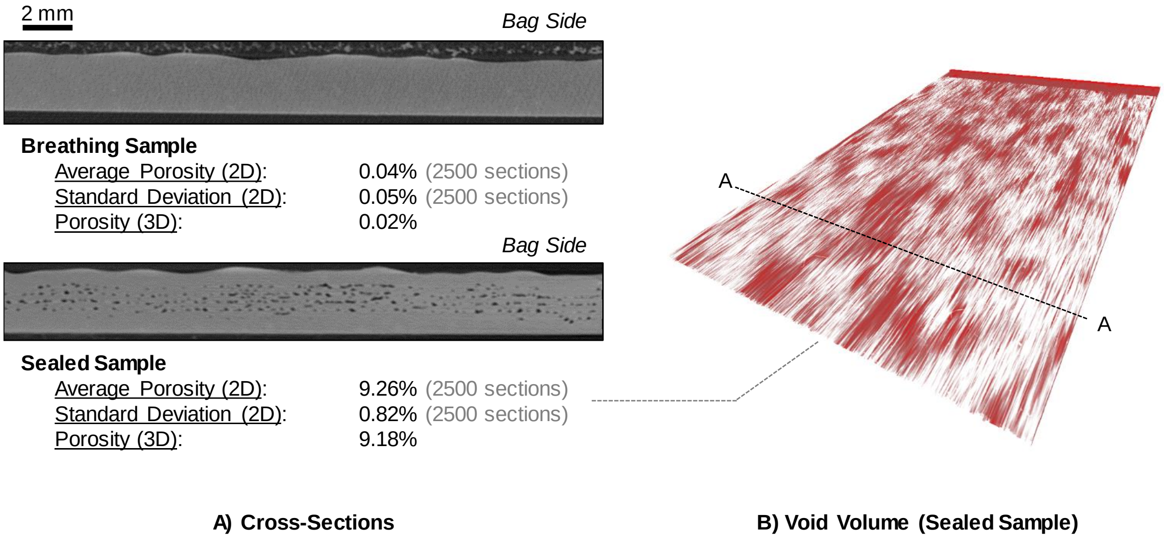

Figure 4: (A) Representative X-ray micrograph regions from the breathing (low defect) and sealed (high defect) samples, along with porosity data acquired using 2D and 3D protocols. (B) Three-dimensional rendering of void volume in sealed sample.

Altogether, these results validate subsequent porosity calculations using light microscopy of large polished cross-sections oriented perpendicular to the fiber direction. Moreover, they provide useful information about defect morphology, and about the range of void contents separating ideally-cured laminates from parts with restricted air evacuation.

Microstructure. Figure 5 shows light micrographs of representative low and high defect microstructures, associated with the sealed region of laminates cured under a high thermal gradient, at 100% vacuum quality, using cold-side breathing (Figure 5A) and hot-side breathing (Figure 5B). The microstructure in Figure 5A exhibits no voids and few defects other than ply waviness. Conversely, Figure 5B exhibits macro-porosity in resin-rich interlaminar regions as well as micro-porosity within the fiber tows, between individual carbon fibers, for an overall areal void content approaching 10%.

Please cite the article as: T. Centea, G. Peters, K. Hendrie and S.R. Nutt, **"Effects of Thermal Gradients on Defect Formation During Consolidation of Partially-Impregnated Prepregs"** J. Compos Mat 51 [28] (2017) 3987-4003 DOI: **10.1177/0021998317733317**

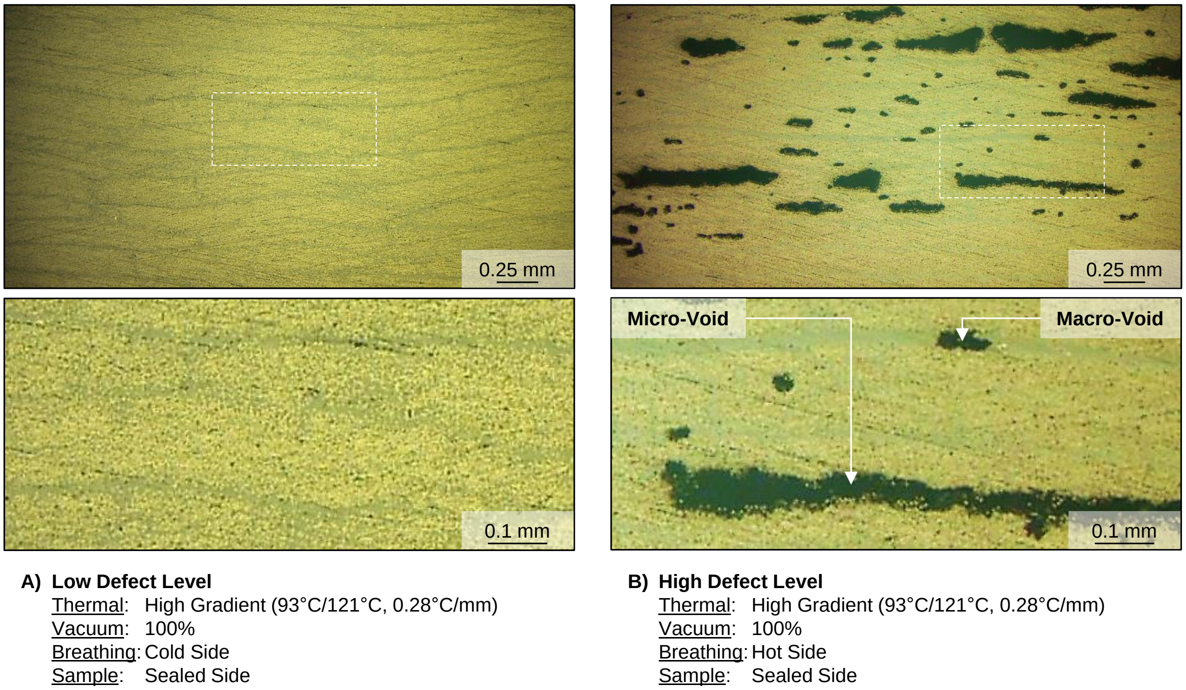

Figure 5: Light micrographs showing representative (A) low defect and (B) high defect microstructures.

Figure 6A shows a scatter plot of measured void contents as a function of vacuum quality and location (breathing edge, middle, or sealed edge). These results do not distinguish between thermal conditions. However, they highlight the substantial influence of vacuum quality on microstructure and, more importantly, show that both low defect (< 2%) and high defect (5-10%) parts can be fabricated at all vacuum levels. Laminates cured under 100% vacuum generally exhibited void contents below 2%, and often below 1%. Parts fabricated at 75% vacuum generally presented porosity between 1% and 6%. Laminates manufactured with only 25% vacuum were also associated with void contents between 1% and 6%, though with higher dispersion. Porosity values were generally lowest within breathing regions, and highest within sealed regions, supporting the prevailing theory that in-plane air evacuation towards the perimeter is the critical defect control mechanism during VBO prepreg processing [4].

Please cite the article as: T. Centea, G. Peters, K. Hendrie and S.R. Nutt, **"Effects of Thermal Gradients on Defect Formation During Consolidation of Partially-Impregnated Prepregs"** J. Compos Mat 51 [28] (2017) 3987-4003 DOI: **10.1177/0021998317733317**

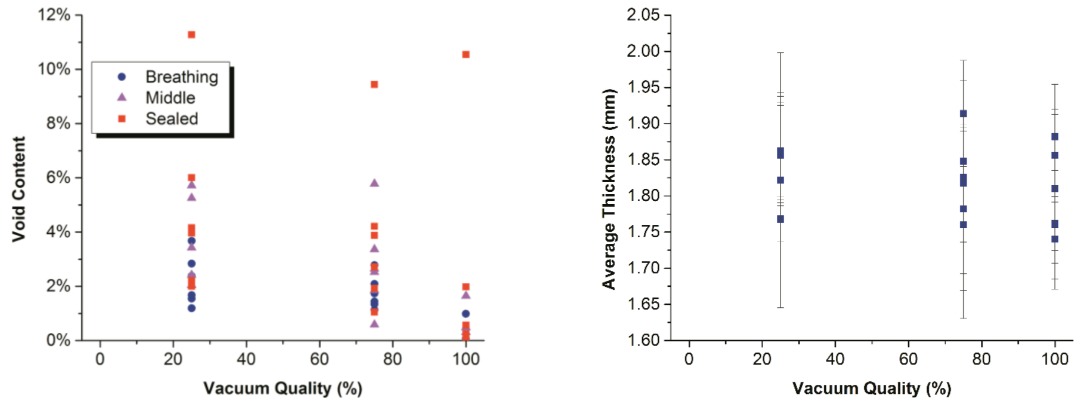

A) Void Content B) Average Thickness

Figure 6: (A) Void content and (B) average thickness for the manufactured samples. The error bars in B) denote one standard deviation.

However, each vacuum level also led to a high porosity (~10%) sample extracted from a sealed region. Porosity data will be analyzed in more detail below. Figure 6B compiles average thickness measurements for each laminate. The results do not differentiate between breathing, middle and sealed regions, resulting in high dispersion. For this unidirectional prepreg, reducing the compaction pressure from intermediate (75%) to low (25%) levels did not lead to a significant increase in cured ply thickness, indicating that the fiber bed architecture is initially compacted to a level similar to 75 kPa. This finding is also consistent with the similar porosity values measured for 75% and 25% vacuum levels. However, the results show that laminates manufactured at 100% vacuum quality exhibited higher consolidation uniformity, or lower thickness variability. The polished micrographs did not show evidence of layup-induced defects such as wrinkles, indicating that the results in Figure 6B are associated with the fiber bed compaction and porosity within the unidirectional laminates.

Please cite the article as: T. Centea, G. Peters, K. Hendrie and S.R. Nutt, **“Effects of Thermal Gradients on Defect Formation During Consolidation of Partially-Impregnated Prepregs”** J. Compos Mat 51 [28] (2017) 3987-4003 DOI: **10.1177/0021998317733317**

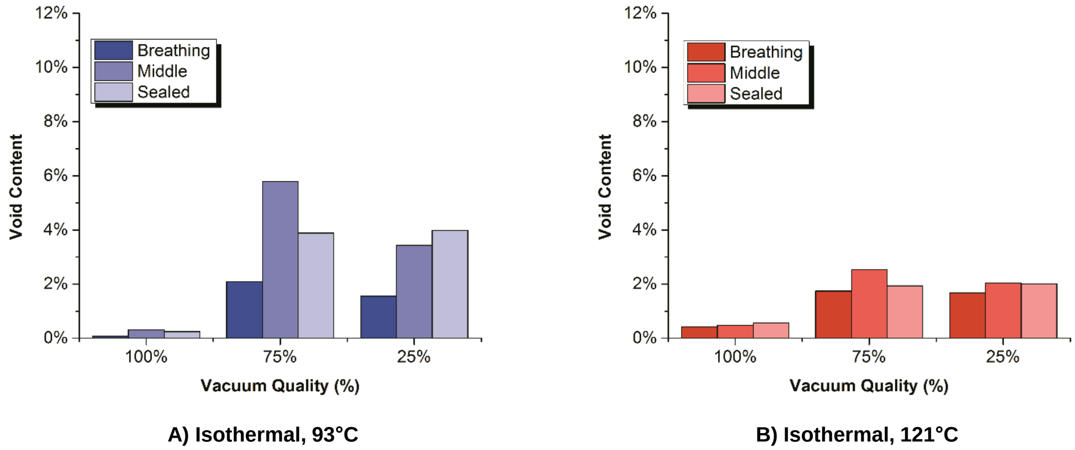

Figure 7: Void contents measured in laminates cured under isothermal conditions at (A) 93°C and (B) 121°C.

Figure 7 shows the void contents measured for parts cured under isothermal conditions (93°C or 121°C) at the three vacuum levels, within the breathing, middle, and sealed regions. Laminates produced isothermally at 100% vacuum contained less than 1% porosity, confirming that high microstructural quality can be achieved using either dwell temperature, provided air is sufficiently evacuated. These results are well-aligned with published data associated with this prepreg material [29,35]. Reduced vacuum levels led to higher porosity at both temperatures, ranging from 2% - 6% at 93°C and 1.5% - 3% at 121°C. The lower defect levels associated with higher-temperature cure are attributed to the lower viscosity of the resin. Recently, Hu et al. reported that the rate of migration of entrapped air bubbles is strongly correlated to the instantaneous temperature [36]. Consequently, cure cycles resulting in lower viscosity enable more rapid bubble movement towards permeable, internal evacuation channels and/or the laminate perimeter. Note, however, that while higher rates of air migration favor air evacuation, gas transport is unlikely to affect the distribution of the solid fiber phase, since it most likely occurs in the creeping regime, with minimal inertial effects. Generally, defect levels were lowest in breathing regions, and comparable in middle and sealed sections, in agreement with the direction of air evacuation. These results provide a detailed baseline of void content and distribution against which to evaluate the effects of non-uniform temperature fields.

Figure 8 and Figure 9 show measured void contents for laminates cured under in-plane thermal gradients as a function of vacuum quality, laminate location, and thermal gradient magnitude, as well as the difference in quality compared to the isothermal baselines. The results are separated according to cold-side breathing (Figure 8) and hot-side breathing (Figure 9). In both cases, the floating columns indicate the porosity range for corresponding isothermally-cured samples, while the bottom graphs show the percentage difference relative to the average void content measured in isothermal laminates.

Figures 8A and 8B relate to cold-side breathing. At full vacuum, void contents were negligible for both small (0.09°C/mm) and large (0.28°C/mm) thermal gradients, and at all locations. At 75% vacuum, cold-side breathing resulted in consistently lower porosity levels than isothermal cure, with reductions of 0.25 – 2% for the 0.09°C/mm gradient and 0.25 - 3.5% for 0.28°C/mm. The 25% vacuum level produced mixed results, with a reduction in void content of ~ 0.5% observed in the middle location, but an increase of 1% in breathing and sealed regions. Overall, the results indicate that cold-side breathing most often mitigates porosity relative to cure at uniform temperature, and that larger gradients accentuate this effect.

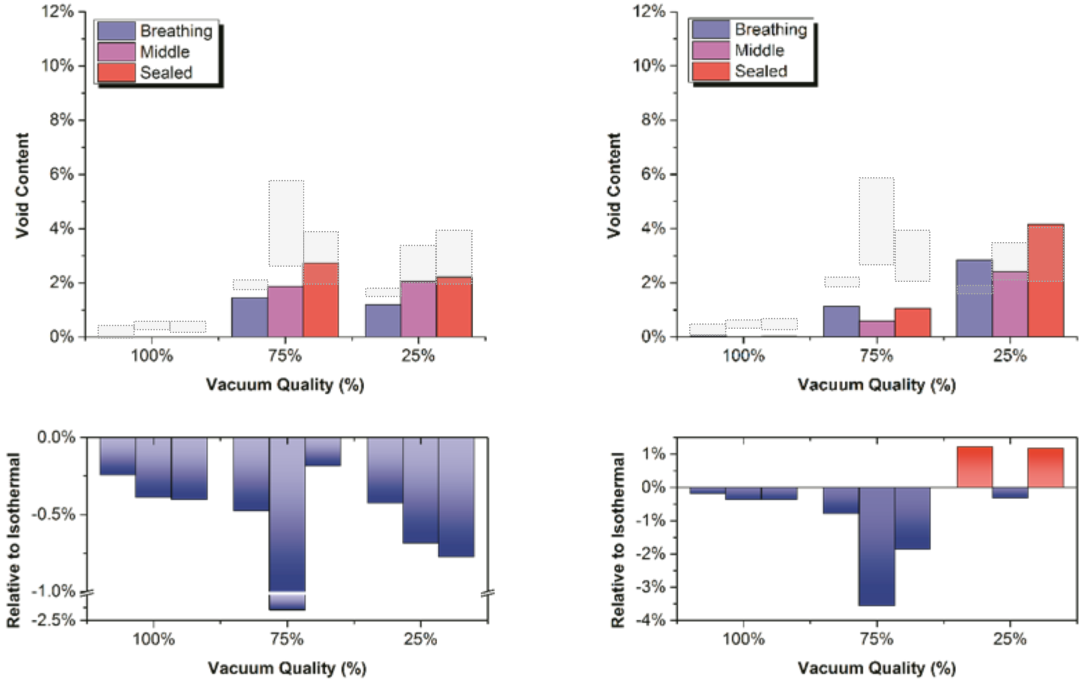

A) Low Thermal Gradient (0.09°C/mm)
Cold-Side Breathing

B) High Thermal Gradient (0.28°C/mm)
Cold-Side Breathing

Figure 8: Void content versus vacuum quality and laminate location for (A) low thermal gradient, cold-side breathing, and (B) high thermal gradient, cold-side breathing, The floating columns indicate the void content range measured at the same location within samples cured isothermally at the same vacuum quality. The bottom graphs highlight the observed trends by showing the percentage point decrease relative to the isothermal case for each column.

Figures 9A and 9B relate to hot-side breathing, and indicate that, in contrast to cold-side breathing, higher edge temperatures most often resulted in large increases in porosity. At full vacuum, the small thermal gradient (0.09°C/mm) led to negligible void contents in breathing and middle regions, but substantial porosity (2%) in the sealed region. Conversely, the large gradient (0.28°C/mm) resulted in 1 – 2% porosity in breathing and central regions, and up to 10% porosity in the sealed region (in close agreement with the fully-sealed, isothermally-cured reference sample analyzed using micro-CT).

Please cite the article as: T. Centea, G. Peters, K. Hendrie and S.R. Nutt, **“Effects of Thermal Gradients on Defect Formation During Consolidation of Partially-Impregnated Prepregs”** J. Compos Mat 51 [28] (2017) 3987-4003 DOI: **10.1177/0021998317733317**

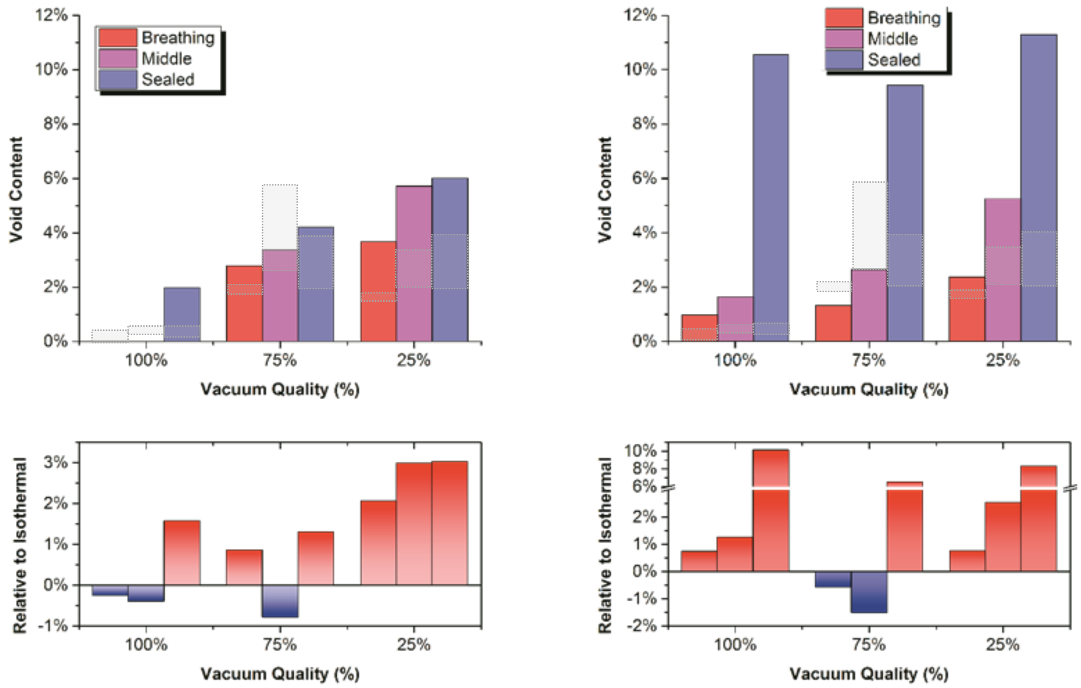

A) Low Thermal Gradient (0.09°C/mm)
Hot-Side Breathing

B) High Thermal Gradient (0.28°C/mm)
Hot-Side Breathing

Figure 9: Void content versus vacuum quality and laminate location for (A) low thermal gradient, hot-side breathing, and (B) high thermal gradient, hot-side breathing, The floating columns indicate the void content range measured at the same location within samples cured isothermally at the same vacuum quality. The bottom graphs highlight the observed trends by showing the percentage point decrease relative to the isothermal case for each column.

Reducing the vacuum level to 75% and 25% led to progressively greater void contents in most cases, with the sole decreases relative to isothermal cure occurring in breathing or middle regions. Altogether, these results show that, for hot-side breathing, larger thermal gradients exacerbate porosity relative to isothermal cure, leading, in some cases, to marked increases in void content.

For hot-side breathing, a porosity gradient was observed within each laminate, with fewest defects in the breathing regions, and most in the sealed regions. This spatial variation was less pronounced for cold-side breathing, being visible in some samples but not in others. However, almost all laminates cured under non-uniform temperatures exhibited lower porosity levels near the breathing edges, consistent with the imposed direction of air evacuation.

Together, Figure 8 and Figure 9 indicate that, for a given vacuum level, thermal gradients can have a profound impact on the amount and distribution of porosity within a cured laminate. The results further show that cold-side breathing can result in reduced porosity (1 - 2%) even with bag pressures of 75 kPa and 25 kPa, but that hot-side breathing can substantially degrade quality relative to isothermal baselines, with sealed-side void contents reaching ~ 10% even when full vacuum is drawn in the bag – an effect comparable to fully sealing the laminate. These results were obtained using unidirectional tape laminates, but the underlying physical mechanisms (discussed below) are likely to occur in all partially-impregnated prepregs.

Figure 10 presents the same laminate void content data as a function of thermal gradient magnitude for cold-side and hot-side breathing cases. Figure 10A shows that, for cold-side breathing, increasing gradient levels led to higher laminate quality for all but a single laminate (25% vacuum quality). Conversely, Figure 10B demonstrates that, for hot-side breathing, steeper gradients increased net defect levels, with highest degradation occurring within the coldest, sealed regions. For simple cases of unidirectional thermal gradients and air evacuation, Figure 10 can act as a process map (for this material and curing conditions) by providing an estimate of void content improvement or knock-down as a function of gradient magnitude and vacuum level.

Please cite the article as: T. Centea, G. Peters, K. Hendrie and S.R. Nutt, **"Effects of Thermal Gradients on Defect Formation During Consolidation of Partially-Impregnated Prepregs"** J. Compos Mat 51 [28] (2017) 3987-4003 DOI: **10.1177/0021998317733317**

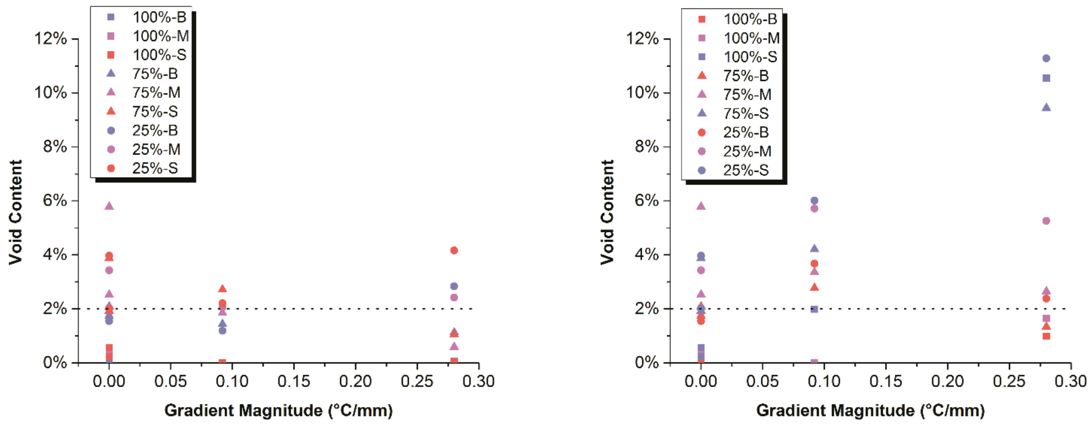

A) Cold-Side Breathing

B) Hot-Side Breathing

Figure 10: Void content versus thermal gradient for laminates fabricated using (A) cold-side breathing and (B) hot-side breathing. The legend labels indicate the vacuum level and laminate region (B = breathing, M = middle or S = sealed).

Discussion

Mechanism. The results presented above demonstrate that thermal gradients and air evacuation are strongly coupled, and can increase or reduce defect levels relative to traditional isothermal cure. The physical mechanism is shown schematically in Figure 11 for the simple case of unidirectional air evacuation and thermal gradients. Non-uniform temperature fields that result in cold-side breathing facilitate air evacuation (Figure 11A). Resin infiltration first occurs within the higher-temperature, sealed region due to the lower viscosity (t_1 to t_2). The low-viscosity resin enables movement of entrapped air bubbles, while the flow front carries bubbles towards the internal evacuation channels and the colder, breathing side, which is less impregnated and more permeable. As the colder side begins to impregnate, the same phenomena facilitate gas transport towards the breathing edge, rather than toward the now-saturated hot region (t_2 to t_3).

Please cite the article as: T. Centea, G. Peters, K. Hendrie and S.R. Nutt, **"Effects of Thermal Gradients on Defect Formation During Consolidation of Partially-Impregnated Prepregs"** J. Compos Mat 51 [28] (2017) 3987-4003 DOI: **10.1177/0021998317733317**

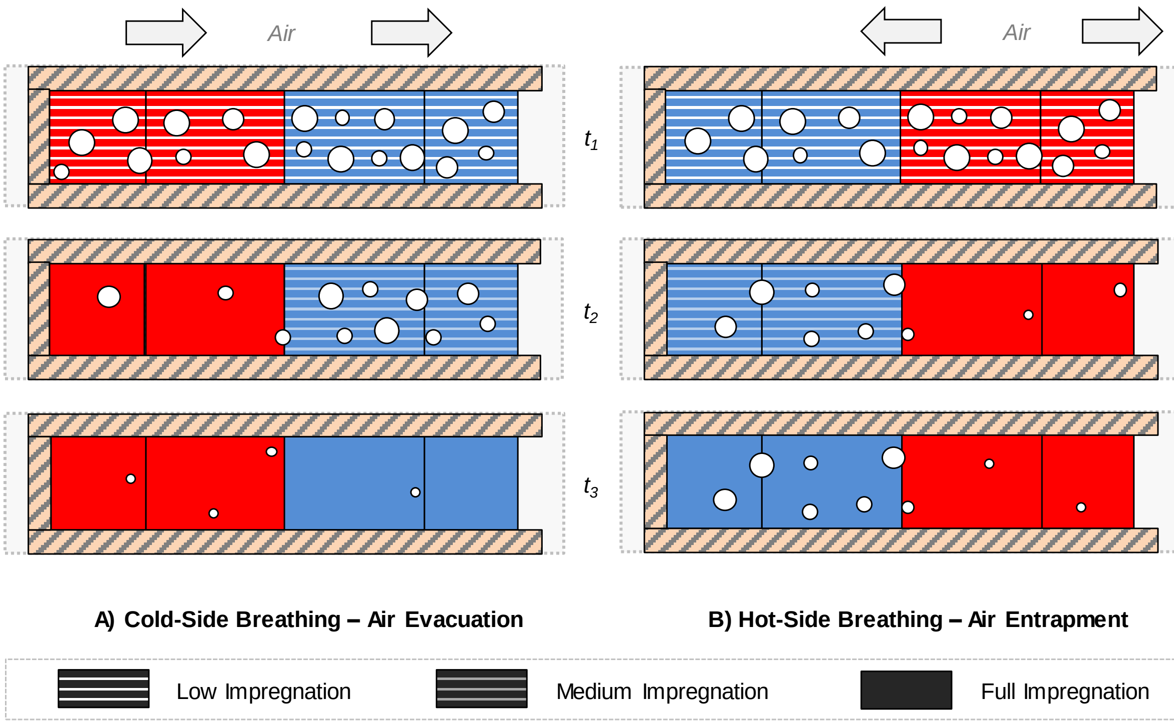

Figure 11: Schematics of (A) favorable cold-side breathing and (B) unfavorable hot-side breathing conditions for the simple case of coupled unidirectional thermal gradients and air evacuation. For simplicity, air within the laminates (entrapped as bubbles or as gas within dry, porous regions) is shown qualitatively as circular "particles." The level of impregnation of each laminate region is indicated using horizontal line textures. The arrows indicate the direction of air evacuation and bubble migration.

In contrast, thermal gradients that lead to hot-side breathing impede air evacuation (Figure 11B). In such cases, consolidation begins first within the breathing region of the laminate. While low resin viscosity conditions and infiltration flow allow some entrapped voids to reach the breathing edge (explaining the relatively low breathing-side porosity within some hot-side breathing laminates in Figure 9), a non-negligible amount of entrapped air may remain (or be driven into) in the colder, still-permeable, sealed side, residing within the micro-porous tows or in the form of entrapped air bubbles surrounded by viscous resin (t_1 to t_2). The impregnation and gelation of the hot-breathing side progressively seal the cold side, inhibiting further air extraction and leading to high levels of gas-induced porosity (t_2 to t_3). The extent of coupling between air evacuation and resin flow, and the magnitude of its impact on part quality, depends on material, process, and part factors, including laminate permeability, temperature cycle, thermal gradient magnitude and direction, and vacuum quality. However, the results presented here indicate that localized hot or cold regions resulting in even a ~10 min discrepancy in prepreg impregnation time (as estimated by our simple model) can markedly alter the amount and distribution of porosity for a wide range of conditions.

Manufacturing Considerations. Thermal gradient-induced defect formation can be eliminated in principle by maximizing air evacuation through high vacuum quality and sufficiently-long air evacuation dwell times, and by minimizing thermal gradients through appropriate part design, tool design, and cure environment selection and control. However, in many cases, sub-optimal manufacturing conditions are unavoidable. Non-uniform temperature fields are commonly encountered during the production of large parts due to variations in laminate thickness, complex tool geometries, or uneven heat inputs from the curing environment. Similarly, lower vacuum conditions may also arise when pumps are shared between multiple parts and bags are improperly sealed, and the consolidation pressure might be reduced if atmospheric pressure is lower than at sea level. Finally, complete air removal is often impossible for large parts due to long breathe-out distances, limits on time available for room-temperature vacuum holding, or the presence of restrictive features such as embedded ply terminations. The current study demonstrates that these conditions can be deliberately manipulated to improve part quality.

During autoclave or oven cure – or, potentially, during pre-cure routines such as hot or cold debulking, or heat-assisted placement of material – temperature distributions within parts can be influenced by modifying the flow of the convective medium, imparting heat locally through blankets or other spot heaters, and/or altering the design of the tool. This study shows that modifications leading to colder-than-average laminate boundaries are beneficial to part quality, particularly if air evacuation is challenging.

Advanced curing environments capable of local heat transfer control can be used to impose uniform temperatures even for parts with challenging geometries. Moreover, such environments enable the use of non-standard thermal cycles: multi-zone heated tooling can be used to create steady-state non-uniform temperature distributions that counteract the detrimental effects of reduced vacuum quality, and lead to high quality parts in conditions that would otherwise result in unacceptable defect levels and part rejection. The findings described in this work isolate and clarify previously undiscussed phenomena, support the increased use of heated tooling, and demonstrate that OOA prepreg processing can derive tangible benefits from out-of-oven curing.

Limitations. The data presented in this study was obtained through lab-scale experiments designed to highlight and clarify the relationships between material properties, process parameters and final part quality for the simple case of unidirectional temperature and air evacuation. The manufacture of complex structures within realistic curing environments is likely to involve two or three-dimensional thermal gradients, as well as air transport over large distances and through complex boundaries (e.g., inserts, ply drops, cores), precluding the use of simple process maps (e.g., Figure 10) as guidelines, and potentially introducing additional complexity (e.g., multiple thermal boundaries, anisotropic gas and resin flows). In such cases, two prospective developments can enhance manufacturability. First, the capacity to accurately simulate consolidation and defect formation and identify optimal manufacturing conditions based on material, process parameters, and complex geometry inputs is desirable. Several authors have proposed models that predict

Please cite the article as: T. Centea, G. Peters, K. Hendrie and S.R. Nutt, **"Effects of Thermal Gradients on Defect Formation During Consolidation of Partially-Impregnated Prepregs"** J. Compos Mat 51 [28] (2017) 3987-4003 DOI: **10.1177/0021998317733317**

aspects of the consolidation of OoA prepregs [37–40]. However, a full three-dimensional implementation that captures air removal and void growth/transport phenomena within realistic parts and subject to representative time, layup, and geometry-dependent heat transfer, fiber bed compaction, and resin flow, has not yet been demonstrated. Second, the development of prepreg formats that enable effective air evacuation in the out-of-plane direction can eliminate the sealing effects of hot-side breathing by no longer requiring escaping air to reach the laminate perimeter [41].

CONCLUSIONS

We studied the effect of thermal gradients on the consolidation and microstructural quality of laminates produced from partially-impregnated prepregs. Parts were manufactured using vacuum bag-only cure on a multi-zone heated tool in isothermal and non-uniform temperature conditions while varying the gradient magnitude direction and vacuum quality. Resin properties and the evolution of prepreg impregnation were described, and used to interpret significant variations in the amount and distribution of porosity.

The results highlighted a non-traditional and seldom-discussed defect formation mechanism, showing that resin flow and air removal mechanisms can couple to profoundly affect the cured part microstructure. Temperature gradients involving lower temperatures at the breathing edges of laminates improved quality relative to isothermal baselines, by driving entrapped air towards the part perimeter. In some cases, cold-side breathing allowed high-quality parts to be fabricated under typically-challenging manufacturing conditions, such as reduced vacuum quality. Conversely, gradients that led to hotter-than-average breathing edges effectively sealed the laminate, preventing air removal, and markedly increased porosity within inner regions, even when full vacuum was drawn within the bag. These results are consistent with reports indicating that air

Please cite the article as: T. Centea, G. Peters, K. Hendrie and S.R. Nutt, **“Effects of Thermal Gradients on Defect Formation During Consolidation of Partially-Impregnated Prepregs”** J. Compos Mat 51 [28] (2017) 3987-4003 DOI: **10.1177/0021998317733317**

evacuation is critical to defect suppression. However, they also show that part quality is highly dependent on (and controlled by) the spatial evolution of temperature, resin flow, permeability, and capacity for bubble transport. These findings were demonstrated using VBO prepregs, but may be relevant to other manufacturing processes reliant on air evacuation and impregnation under a vacuum bag, including RFI and VARI/RIFT, provided that air evacuation and resin flow are coupled over similar time and length scales.

The ongoing transition towards out-of-autoclave manufacturing provides opportunities to evaluate advanced processing environments and curing strategies. The multi-zone heated tool used in this study leverages the ability to fabricate parts without a pressurized vessel, and can be used to impose thermal cycles that cannot be achieved using convective heating. The effects of non-uniform heating on other part quality and performance metrics, including residual stresses and mechanical response, should be evaluated. However, such advanced infrastructure affords intriguing prospects for controlling part quality and raising manufacturing efficiency.

APPENDIX – TOW IMPREGNATION MODEL

Model Development. Partially-impregnated prepregs designed for OOA processing typically consist of a fiber bed located between two continuous resin films. Following layup and compaction, macro-pore spaces surrounding the tows are saturated with resin. Therefore, tow impregnation is the key flow process occurring during cure. Several models have been developed to describe resin infiltration during VBO prepreg cure [33,37,38,42]. Here, a simple approach was used to estimate typical impregnation times as a function of temperature [33].

Resin infiltration into dry fiber tows consists of the low Reynolds number flow of a viscous fluid within a porous medium, and can be described by continuity equations for solid and fluid phases and the Darcy's Law description of momentum balance. These equations can be simplified by assuming that, during infiltration, dry fiber bed regions ahead of the resin flow front are compressed to a constant volume fraction V_f and that the pore spaces behind the flow front are rigid and fully saturated with resin. This simplification eliminates the coupling between resin pressure and fiber bed compaction, and subsequent relaxation of the fiber bed in impregnated regions. However, the degree of impregnation, rather than the fiber volume fraction in saturated regions, is the key material state variable during VBO cure. Hence, simple models can provide useful estimates of dominant phenomena associated with part quality. The resulting problem is described by the following equations:

$$\overline{v_r} = -\frac{\overline{\overline{\overline{K}}}}{\mu\left(1 - V_f\right)} \nabla P \qquad \text{A.1}$$

$$\nabla \cdot \overline{v_r} = 0 \qquad \text{A.2}$$

In Eq. (A.1), $\overline{v_r}$ is the average local velocity of the resin within the pore volume, $\overline{\overline{\overline{K}}}$ is the permeability tensor of the tow, μ is the resin viscosity, V_f is the tow fiber volume fraction, and P is the resin pressure.

Microstructural images of partially-impregnated unidirectional prepregs reveal that the dry tow cores are planar, and that infiltration occurs mainly in the transverse direction [33,43]. For such a fiber bed architecture, tow impregnation can therefore be approximated using a linear, one-directional infiltration model. Thus, Eq. (A.1) and (A.2) simplify to the following forms, where the subscript x denotes the direction of flow:

$$v_x = -\frac{K_x}{\mu(1 - V_f)} \frac{\partial P}{\partial x} \qquad \text{A.3}$$

$$\frac{\partial v_x}{\partial x} = 0 \qquad \text{A.4}$$

Resin flow is assumed to be driven by a far-field resin pressure P_r outside the tow ($x = 0$) and resisted by a pressure P_f at the flow front ($x = x_f$). Combining Eq. (A.3) and (A.4), solving for the linear pressure field, and re-inserting the $P(x)$ equation into Eq. (A.3) yields the 1D solution for Darcy flow within a porous medium:

$$v_x = \frac{K_x}{\mu(1 - V_f)} \left[\frac{P_r - P_f}{x_f}\right] \qquad \text{A.5}$$

Finally, Eq. (A.5) may be non-dimensionalized by defining a degree of tow impregnation $\beta = x_f/L$, where L is the total flow length. The rate of tow impregnation is therefore:

$$\frac{d\beta}{dt} = \frac{1}{L}\left(\frac{\partial x_f}{dt}\right) \qquad \text{A.6}$$

$$\frac{d\beta}{dt} = \frac{K_x}{\mu(1 - V_f)} \left[\frac{P_r - P_f}{\beta L^2}\right] \qquad \text{A.7}$$

Eq. (A.7) can be solved using a simple forward-Euler numerical scheme while varying the resin viscosity μ at each time step. The constants K_x, V_f, P_r, P_f and L must be identified.

Parameter Identification. The viscosity μ of the 5320-1 resin was calculated for any time-temperature profile using the predictive models developed by Kim et al. [28], assuming an out-time of four days. Tow properties and impregnation rates were determined according to the method described in Ref. [33]. Laminates were partially processed using a cure cycle consisting of a 2°C/min ramp to 121°C, with parts extracted at 70°C, 80°C, and 90°C. Next, samples from each laminate were cold-cured in an ammonia environment (following the protocol described by Howard [44]), polished, and inspected using a light microscope. The cured ply thickness t_{CP} was measured as 0.150 mm, resulting in a flow length L of 0.075 mm. The fiber volume fraction V_f within a single ply was calculated using t_{CP} and the following equation, assuming a fiber bed areal weight A_w of 145 g/m^2 and a fiber density ρ_f of 1770 kg/m^3:

$$V_f = \frac{A_w}{(t_{CP})(\rho_f)} \qquad \text{A.8}$$

The driving and resisting resin pressures were selected based on the guidelines provided in Ref. [33]. The driving resin pressure P_r was set to 101 300 Pa, or the maximum achievable under vacuum compaction. The resisting resin pressure was set to 0 Pa, assuming full air evacuation as well as negligible wetting effects, since the fiber volume fraction predicted by Eq. (A.8), 0.55, does not meet the criterion for spontaneous capillary infiltration cited by Foley and Gillespie [45].

Finally, as in Centea and Hubert [33], the permeability K_x was used to fit the model to measured impregnation data for a known cure cycle. The level of tow impregnation in the partially processed laminates was measured using image analysis by calculating the ratio of dry fiber tow area to total

Please cite the article as: T. Centea, G. Peters, K. Hendrie and S.R. Nutt, **"Effects of Thermal Gradients on Defect Formation During Consolidation of Partially-Impregnated Prepregs"** J. Compos Mat 51 [28] (2017) 3987-4003 DOI: **10.1177/0021998317733317**

tow area. Next, model predictions were computed for the same time-temperature cycle, and a least-squares fit was used to identify an appropriate permeability. The measured data and predicted values are shown in Figure 12. The calculated permeability is relatively low for the calculated volume fraction. However, the calculation provides an accurate prediction of the evolution of impregnation, and remains within a physically-feasible range for VBO prepregs.

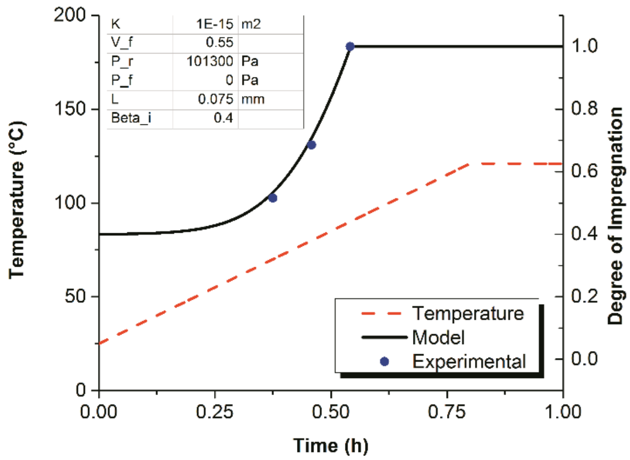

Figure 12: Predicted and measured degree of impregnation for a calibration cure cycle, with model parameters (inset).

ACKNOWLEDGEMENTS

This work was supported by the National Science Foundation through the G8 Interdisciplinary Initiative on Materials Efficiency project titled "Sustainable Manufacturing Using Out-of-Autoclave Prepregs" (CMMI-1229011) and by the M.C. Gill Composites Center at the University of Southern California. The authors are grateful for guidance from the project's industrial advisory board. The prepregs and consumables were generously donated by Cytec Industries and Airtech

International, respectively. Finally, Wei Hu carried out the partial processing and cold cure of the samples used to develop the tow impregnation model.

REFERENCES

1. Campbell FC. Manufacturing Technology for Aerospace Structural Materials. London: Elsevier; 2006.

2. Witik RA, Gaille F, Teuscher R, Ringwald H, Michaud V, Månson J-AE. Economic and environmental assessment of alternative production methods for composite aircraft components. *J Clean Prod [Internet]*. 2012 Jul;29–30(0):91–102. Available from: http://www.sciencedirect.com/science/article/pii/S0959652612001047

3. Michaud V, Mortensen A. Infiltration processing of fibre reinforced composites: governing phenomena. *Compos Part A Appl Sci Manuf [Internet]*. 2001;32(8):981–996. Available from: http://www.sciencedirect.com/science/article/B6TWN-43DF042-2/2/771eeda5b364c8d96e6edb924a050fd3

4. Centea T, Grunenfelder LK, Nutt SR. A review of out-of-autoclave prepregs - material properties, process phenomena and manufacturing considerations. *Compos Part A Appl Sci Manuf [Internet]*. 2015 Oct [cited 2014 Oct 23];70:132–154. Available from: http://www.sciencedirect.com/science/article/pii/S1359835X14003108

5. Bogetti TA, Gillespie JW. J. Two-Dimensional Cure Simulation of Thick Thermosetting Composites. *J Compos Mater [Internet]*. 1991 Mar 1 [cited 2016 May 4];25(3):239–273. Available from: http://jcm.sagepub.com/content/25/3/239.short

6. Bogetti TA, Gillespie JW. Process-Induced Stress and Deformation in Thick-Section Thermoset Composite Laminates. *J Compos Mater [Internet]*. 1992 Jan 1 [cited 2016 May 4];26(5):626–660. Available from: http://jcm.sagepub.com/content/26/5/626.short

7. Hubert P, Vaziri R, Poursartip A. A two-dimensional flow model for the process simulation of complex shape composite laminates. *Int J Numer Methods Eng [Internet]*. 1999;44(1):1–26. Available from: http://dx.doi.org/10.1002/(SICI)1097-0207(19990110)44:1%3C1::AID-NME481%3E3.0.CO;2-K

8. Bruschke M V., Advani SG. A numerical approach to model non-isothermal viscous flow through fibrous media with free surfaces. *Int J Numer Methods Fluids [Internet]*. 1994 Oct 15 [cited 2016 Apr 6];19(7):575–603. Available from: http://doi.wiley.com/10.1002/fld.1650190704

9. Mal O, Couniot A, Dupret F. Non-isothermal simulation of the resin transfer moulding press. *Compos Part A Appl Sci Manuf [Internet]*. 1998 Jan [cited 2016 May 4];29(1–2):189–198. Available from: http://www.sciencedirect.com/science/article/pii/S1359835X97000651

10. Ngo ND, Tamma KK. Non-isothermal "2-D flow/3-D thermal" developments encompassing process modelling of composites: flow/thermal/cure formulations and validations. *Int J Numer Methods Eng [Internet]*. 2001 Mar 10 [cited 2016 May 4];50(7):1559–1585. Available from: http://doi.wiley.com/10.1002/nme.85

11. Park CH, Saouab A, Bréard J, Han WS, Vautrin A, Lee W Il. An integrated optimisation for the weight, the structural performance and the cost of composite structures. *Compos Sci Technol [Internet]*. 2009 Jun [cited 2014 Jul 17];69(7–8):1101–1107. Available from: http://www.sciencedirect.com/science/article/pii/S0266353809000517

12. Shojaei A. Simulation of the three-dimensional non-isothermal mold filling process in resin transfer

molding. *Compos Sci Technol [Internet]*. 2003 Oct [cited 2016 May 4];63(13):1931–1948. Available from: http://www.sciencedirect.com/science/article/pii/S0266353803001611

13. Abbassi A, Shahnazari M. Numerical modeling of mold filling and curing in non-isothermal RTM process. *Appl Therm Eng [Internet]*. 2004 Nov [cited 2016 May 4];24(16):2453–2465. Available from: http://www.sciencedirect.com/science/article/pii/S1359431104000729

14. Young W-B. Three-dimensional nonisothermal mold filling simulations in resin transfer molding. *Polym Compos [Internet]*. 1994 Apr [cited 2016 Apr 6];15(2):118–127. Available from: http://doi.wiley.com/10.1002/pc.750150205

15. Antonucci V, Giordano M, Nicolais L, Di Vita G. A simulation of the non-isothermal resin transfer molding process. *Polym Eng Sci [Internet]*. 2000 Dec [cited 2016 May 4];40(12):2471–2481. Available from: http://doi.wiley.com/10.1002/pen.11378

16. Antonucci V, Giordano M, Hsiao K-T, Advani SG. A methodology to reduce thermal gradients due to the exothermic reactions in composites processing. *Int J Heat Mass Transf [Internet]*. 2002 Apr [cited 2016 Apr 6];45(8):1675–1684. Available from: http://www.sciencedirect.com/science/article/pii/S0017931001002666

17. Shi F, Dong X. 3D numerical simulation of filling and curing processes in non-isothermal RTM process cycle. *Finite Elem Anal Des [Internet]*. 2011 Jul [cited 2016 May 4];47(7):764–770. Available from: http://www.sciencedirect.com/science/article/pii/S0168874X11000345

18. Fahrang L, Fernlund G. Void evolution and gas transport during cure in out-of-autoclave prepreg laminates. In: Proceedings of the SAMPE 2011 Conference. Long Beach, CA.: Society for the Advancement of Materials and Process Engineering; 2011.

19. Black S. Tooling for composites: Evolutionary trajectory [Internet]. *High Perform. Compos.* 2011

Jul [cited 2016 Jun 21];Available from: http://www.compositesworld.com/articles/tooling-for-composites-evolutionary-trajectory

20. Centea T, Nutt SR. Manufacturing cost relationships for vacuum bag-only prepreg processing. *J Compos Mater [Internet]*. 2016 Sep 15 [cited 2015 Sep 29];50(17):2305–2321. Available from: http://jcm.sagepub.com/content/early/2015/09/15/0021998315602949.abstract

21. Arney M, Grove SM, Progoulakis I, Searle T, Short D, Spooner J, et al. Integrally-heated tooling for the manufacture of fibre-reinforced composites. In: Proceedings of the Composites Processing 2004 Conference. Bromsgrove: 2004.

22. Abdalrahman R, Grove S, Kyte A, Rizvi MJ. Numerical simulation and design optimisation of an integrally-heated tool for composite manufacturing. *Mater Des [Internet]*. 2014 Dec [cited 2015 Feb 7];64:477–489. Available from: http://www.sciencedirect.com/science/article/pii/S0261306914005512

23. Abdalrahman R, Grove S, Kyte A, Rizvi MJ. Numerical simulation and experimental verification of heating performance of an integrally water-heated tool. *J Reinf Plast Compos [Internet]*. 2016 Apr 1 [cited 2016 Jul 1];35(8):671–687. Available from: http://jrp.sagepub.com/cgi/doi/10.1177/0731684415626804

24. O'Bradaigh C, Doyle A, Doyle D, Feerick P. Electrically-Heated Ceramic Composite Tooling for Out-of-Autoclave Manufacturing of Large Composite Structures. *SAMPE Journal2*. 11AD;47:6–14.

25. Smith AW, Hubert P, Goyette K, Kazanas C. Development of a Heated Tooling Solution to Improve Process Flexibility for Out-Of-Autoclave Prepregs. In: Proceedings of the 45th International SAMPE Technical Conference. Wichita, KS: Society for the Advancement of Materials and Process Engineering; 2013.

Please cite the article as: T. Centea, G. Peters, K. Hendrie and S.R. Nutt, **"Effects of Thermal Gradients on Defect Formation During Consolidation of Partially-Impregnated Prepregs"** J. Compos Mat 51 [28] (2017) 3987-4003 DOI: **10.1177/0021998317733317**

26. Payette S, Smith AW, Goyette K, Kazanas C, Hubert P. Out-Of-Autoclave Manufacturing: Benchmarking of an Integrally Heated Tool-Plate. In: Proceedings of the Composites and Advanced Materials Expo (CAMx). Orlando, FL: Society for the Advancement of Material and Process Engineering; 2014.

27. Schuetze-Coburn A, Klimkzak S, Tsui V. Development of Active Tooling for Composite Manufacturing. In: Proceedings of the AIAA Region VI Student Conference. Sacramento, CA: American Institute for Aeronautics and Astronautics; 2014.

28. Kim D, Centea T, Nutt SR. Out-time effects on cure kinetics and viscosity for an out-of-autoclave (OOA) prepreg: Modelling and monitoring. *Compos Sci Technol [Internet]*. 2014 Jun [cited 2014 Jun 12];100:63–69. Available from: http://www.sciencedirect.com/science/article/pii/S0266353814001742

29. Centea T, Hubert P. Out-of-autoclave prepreg consolidation under deficient pressure conditions. *J Compos Mater [Internet]*. 2014 Jul 8;48(16):2033–2045. Available from: http://jcm.sagepub.com/content/early/2013/07/04/0021998313494101.abstract

30. Kratz J, Hubert P. Anisotropic air permeability in out-of-autoclave prepregs: Effect on honeycomb panel evacuation prior to cure. *Compos Part A Appl Sci Manuf [Internet]*. 2013 Jun;49(0):179–191. Available from: http://www.sciencedirect.com/science/article/pii/S1359835X13000687

31. Grunenfelder LK, Centea T, Hubert P, Nutt SR. Effect of room-temperature out-time on tow impregnation in an out-of-autoclave prepreg. *Compos Part A Appl Sci Manuf [Internet]*. 2013;45(0):119–126. Available from: http://www.sciencedirect.com/science/article/pii/S1359835X12003053

32. Centea T, Hughes SM, Payette S, Kratz J, Hubert P. Scaling Challenges Encountered with Out-of-

Autoclave Prepregs. In: Proceedings of the 53rd AIAA/ASME/ASCE/AHS/ASC Structures, Structural Dynamics and Materials Conference. Honolulu, HI: American Institute for Aeronautics and Astronautics; 2012.

33. Centea T, Hubert P. Modelling the effect of material properties and process parameters on tow impregnation in out-of-autoclave prepregs. *Compos Part A Appl Sci Manuf [Internet]*. 2012;43(9):1505–1513. Available from: http://www.sciencedirect.com/science/article/pii/S1359835X12001212?v=s5

34. Hamill L, Centea T, Nutt S. Surface porosity during vacuum bag-only prepreg processing: Causes and mitigation strategies. *Compos Part A Appl Sci Manuf [Internet]*. 2015 Aug [cited 2015 May 28];75:1–10. Available from: http://www.sciencedirect.com/science/article/pii/S1359835X15001347

35. Centea T, Hughes S-M, Payette S, Kratz J, Hubert P. Scaling challenges encountered with out-of-autoclave prepregs. In: Collection of Technical Papers - AIAA/ASME/ASCE/AHS/ASC Structures, Structural Dynamics and Materials Conference. 2012.

36. Hu W, Grunenfelder LK, Nutt SR. In-Situ Observation of Void Transport During Vacuum Bag-Only Cure. In: Proceedings of the SAMPE 2016 Technical Conference. Long Beach, CA: Society for the Advancement of Material and Process Engineering; 2016.

37. Rouhi MS, Wysocki M, Larsson R. Modeling of coupled dual-scale flow–deformation processes in composites manufacturing. *Compos Part A Appl Sci Manuf [Internet]*. 2013;46(0):108–116. Available from: http://www.sciencedirect.com/science/article/pii/S1359835X12003363

38. Helmus R, Centea T, Hubert P, Hinterholzl R. Out-of-autoclave prepreg consolidation: Coupled air evacuation and prepreg impregnation modeling. *J Compos Mater [Internet]*. 2015;Available from: http://jcm.sagepub.com/cgi/doi/10.1177/0021998315592005--

39. Helmus R, Hinterhölzl R, Hubert P. A stochastic approach to model material variation determining tow impregnation in out-of-autoclave prepreg consolidation. *Compos Part A Appl Sci Manuf [Internet]*. 2015 Apr [cited 2015 Jul 19];77:293–300. Available from: http://www.sciencedirect.com/science/article/pii/S1359835X15001104

40. Kourkoutsaki T, Comas-Cardona S, Binetruy C, Upadhyay RK, Hinterhoelzl R. The impact of air evacuation on the impregnation time of Out-of-Autoclave prepregs. *Compos Part A Appl Sci Manuf.* 2015;79:30–42.

41. Grunenfelder LK, Dills A, Centea T, Nutt S. Effect of prepreg format on defect control in out-of-autoclave processing. *Compos Part A Appl Sci Manuf.* 2017;93:88–99.

42. Gangloff JJ, Simacek P, Sinha S, Advani SG. A Process Model For The Compaction And Saturation Of Partially Impregnated Thermoset Prepreg Tapes. *Compos Part A Appl Sci Manuf [Internet]*. 2014 Jun [cited 2014 Jun 11];64. Available from: http://www.sciencedirect.com/science/article/pii/S1359835X14001456

43. Centea T, Hubert P. Measuring the impregnation of an out-of-autoclave prepreg by micro-CT. *Compos Sci Technol [Internet]*. 2011;71(5):593–599. Available from: http://www.sciencedirect.com/science/article/B6TWT-51NG4NW-4/2/0be6ba6c3a67408661571d2f60e23f55

44. Howard S. Evaluating Consolidation Dynamics - Study of Key Consolidation Parameters in a Vacuum Bag Only (VBO) Cure. In: Proceedings of the SAMPE 2016 Technical Conference. Long Beach, CA: Society for the Advancement of Material and Process Engineering; 2016.

45. Foley ME, Gillespie JW. Modeling the Effect of Fiber Diameter and Fiber Bundle Count on Tow Impregnation during Liquid Molding Processes. *J Compos Mater [Internet]*. 2005 Jun;39(12):1045–

1065. Available from: http://jcm.sagepub.com/cgi/content/abstract/39/12/1045

Please cite the article as: T. Centea, G. Peters, K. Hendrie and S.R. Nutt, **“Effects of Thermal Gradients on Defect Formation During Consolidation of Partially-Impregnated Prepregs”** J. Compos Mat 51 [28] (2017) 3987-4003 DOI: **10.1177/0021998317733317**